

Metal- and Ligand-Directed One-Pot Syntheses, Crystal Structures, and Properties of Novel Oxo-Centered Tetra- and Hexametallic Clusters**

Rolf W. Saalfrank,^{*,[a]} Uwe Reimann,^[a] Mareike Göritz,^[a] Frank Hampel,^[a] Andreas Scheurer,^[a] Frank W. Heinemann,^[b] Michael Büschel,^[c] Jörg Daub,^[c] Volker Schünemann,^[d] and Alfred X. Trautwein^[d]

Dedicated to Professor Johann Gasteiger on the occasion of his 60th birthday

Abstract: Starting from closely related metal–ligand combinations, completely different oligomeric metal clusters are synthesized. Whereas, picoline–tetrazolylamide HL^1 (**1**) and zinc or nickel acetate afforded $[2 \times 2]$ grids $[M_4(L^1)_8]$ (**2**), slightly different *N*-(2-methylthiazole-5-yl)-thiazole-2-carboxamide HL^2 (**5a**) and nickel acetate yielded the monometallic complex $[Ni(L^2)_2(OH_2)_2]$ (**6**). In contrast, reaction of **5a** with zinc acetate produced the tetrametallic zinc cluster $[Zn_4O(L^2)_4(OAc)_2]$ (**7**). Even more surprising, when 3-methyl-substituted HL^3 (**5b**) instead of 2-methyl-

substituted HL^2 (**5a**) was allowed to react under identical conditions with zinc acetate, the cluster $[Zn_4O(L^3)_4Cl_2]$ (**8**) crystallized from dichloromethane. Clusters **7** and **8** are isostructural. As for **7**, in **8** two of the edges of the tetrahedron of zinc ions are doubly bridged, two are singly bridged, and the other two are nonbridged. On the other hand, when

iron(II) acetate under aerobic conditions was allowed to react with **5a**, the unprecedented complex $[(Fe_3O(L^2)_2(OAc)_4)_2O]$ (**9**) was isolated. Cluster **9** is composed of two trimetallic, triangular μ_3-O^{2-} -centered $[Fe_3O(L^2)_2(OAc)_4]^+$ modules, linked by an almost linear μ_2-O^{2-} bridge. The Mössbauer spectrum together with cyclic voltammetric and square-wave voltammetric measurements of **9** are reported, and **6–9** were characterized unequivocally by single-crystal X-ray structure analyses.

Keywords: cluster compounds · cyclic voltammetry · Mössbauer spectroscopy · N ligands · self-assembly · supramolecular chemistry

Introduction

The synergistic effect of serendipity and rational design, based on the well-known rules of coordination chemistry make the assembly of metalla-topomers of the classical, mere organic coronates as well as bi- and tricyclic cryptates, possible. Compared with the conventional organic-based N-bridged supramolecular structures,^[1] the new clusters feature metal

ions that act as bridgeheads. Recent developments in the field of design and synthesis of supramolecular inorganic structures that exhibit novel properties have provided exciting new prospects.^[2] In this context, we reported on rectangular tetrametallic clusters $[M_4(L^1)_8]$ (**2**), which were accessible in a one-pot reaction from zinc or nickel acetate and picoline–tetrazolylamide HL^1 (**1**; Scheme 1).^[3] One of the main

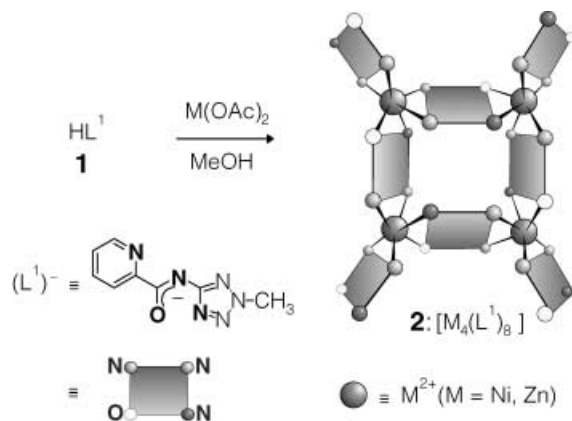
[a] Prof. Dr. R. W. Saalfrank, Dr. U. Reimann, Dipl.-Chem. M. Göritz, Dr. F. Hampel, Dr. A. Scheurer
Institut für Organische Chemie der Universität Erlangen-Nürnberg
Henkestrasse 42, 91054 Erlangen (Germany)
Fax: (+49)9131-852-1165
E-mail: saalfrank@organik.uni-erlangen.de

[b] Dr. F. W. Heinemann
Institut für Anorganische Chemie der Universität Erlangen-Nürnberg
91054 Erlangen (Germany)

[c] Dipl.-Chem. M. Büschel, Prof. Dr. J. Daub
Institut für Organische Chemie der Universität Regensburg
93053 Regensburg (Germany)

[d] Dr. V. Schünemann, Prof. Dr. A. X. Trautwein
Institut für Physik der Medizinischen Universität Lübeck
23538 Lübeck (Germany)

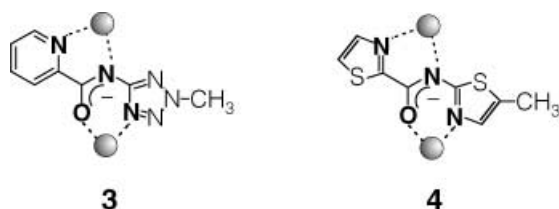
[**] Chelate Complexes, Part 22; for Part 21 see reference [12].



Scheme 1. Synthesis of tetrametallic nickel and zinc clusters $[M_4(L^1)_8]$ (**2**).

structural characteristics of the square $[2 \times 2]$ grids **2** are the two different sets of bonding modes observed for $(L^1)^-$. A set of four tetradentate ligands links two metal ions each by a five-membered chelate ring and a six-membered chelate ring to construct the $[M_4(L^1)_4]^{4+}$ core. In this case $(L^1)^-$ coordinates to one metal ion through the pyridine and the amide nitrogen donors and to the neighboring metal ion through the nitrogen donor of the tetrazolyl group and the oxygen donor of the amide function. In contrast, the four ligands $(L^1)^-$ of the second set exhibit a bidentate bonding mode. These ligands coordinate across the pyridine and the amide nitrogen donors only and complete the slightly distorted octahedral coordination sphere at the metal vertices.

Formal replacement of the pyridine and tetrazole heterocycles in fragment **3** by thiazole rings leads to new fragment **4** (Scheme 2). The geometric requisites of fragments **3** and **4** are very similar and for that reason, we expected that **4** should also be suitable for the generation of square $[2 \times 2]$ grids.

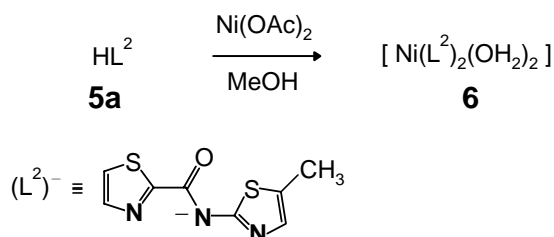


Scheme 2. Schematic representation of the commensurate building blocks **3** and **4** suitable for the construction of cyclic tetrametallic clusters.

Abstract in German: In dieser Arbeit wird, ausgehend von nahe verwandten Metall-Ligand-Kombinationen, die Synthese völlig unterschiedlicher oligomerer Metallcluster beschrieben. Während bei der Umsetzung von Picolin-tetrazolylamid HL^1 **1** und Zink- bzw. Nickelacetat das $[2 \times 2]$ Grid $[M_4(L^1)_8]$ **2** gebildet wurde, entstand bei der Reaktion des nur geringfügig unterschiedlichen N -(2-Methylthiazol-5-yl)-thiazol-2-carboxamids HL^2 **5a** mit Nickelacetat der einkernige Metallkomplex $[Ni(L^2)_2(OH_2)_2]$ **6**. Im Gegensatz dazu isolierten wir bei der Umsetzung von HL^2 **5a** mit Zinkacetat den vierkernigen Zinkcluster $[Zn_4O(L^2)_4(OAc)_2]$ **7**. Noch überraschender war der Befund, dass bei der Reaktion von 3-Methyl- HL^3 **5b** anstelle von 2-Methyl- HL^2 **5a** mit Zinkacetat bei ansonsten identischen Reaktionsbedingungen aus Dichlormethan der Cluster $[Zn_4O(L^3)_4Cl_2]$ **8** kristallisierte. Die Cluster **7** und **8** sind isostrukturell. Wie in **7**, sind auch in **8** zwei Seiten des Zinktetraeders doppelt, zwei einfach und die restlichen zwei nicht überbrückt. Völlig unerwartet lieferte die Umsetzung von Eisen(III)acetat mit HL^2 **5a** unter aeroben Bedingungen den präzedenzlosen Cluster $[Fe_3O(L^2)_2(OAc)_4]_2O$ **9**. Cluster **9** besteht aus zwei μ_3-O^{2-} -zentrierten dreieckigen $[Fe_3O(L^2)_2(OAc)_4]^+$ Bausteinen, die über eine μ_2-O^{2-} -Brücke nahezu linear miteinander verknüpft sind. Wir berichten über das Mößbauer-Spektrum von **9**, sowie über cyclovoltammetrische und square-wave Messungen an dieser Verbindung. Die Strukturen der Cluster **6**, **7**, **8** und **9** wurden eindeutig durch röntgenographische Einkristall Strukturanalysen gesichert.

Results and Discussion

To confirm this hypothesis, we treated HL^2 (**5a**) with nickel(II), zinc(II), and iron(II) acetate. N -(2-Methylthiazole-5-yl)-thiazole-2-carboxamide (**5a**) was prepared according to literature procedures^[4] by coupling of 2-thiazolecarbonyl chloride with methyl-5-aminothiazole in N -methylpyrrolidin-2-one (NMP) in the presence of lithium chloride. Reaction of HL^2 (**5a**) with nickel acetate in methanol led to a dark green precipitate. Contrary to what was expected, the elemental analysis and FAB-MS spectrum identified **6** as a monometallic chelate complex of the composition $[Ni(L^2)_2(OH_2)_2]$ (Scheme 3).



Scheme 3. Synthesis of the mononuclear nickel cluster $[Ni(L^2)_2(OH_2)_2]$ (**6**).

These results were confirmed by an X-ray crystallographic structure analysis. Thus, the two ligands $(L^2)^-$ of *cis*-**6** are bound across the thiazole and amide nitrogen donors and generate five-membered chelate rings. The slightly distorted octahedral coordination sphere at the nickel center is completed by oxygen donors of two water molecules which form extra hydrogen bonds each to the nitrogen atom of the methylthiazole groups (Figure 1).

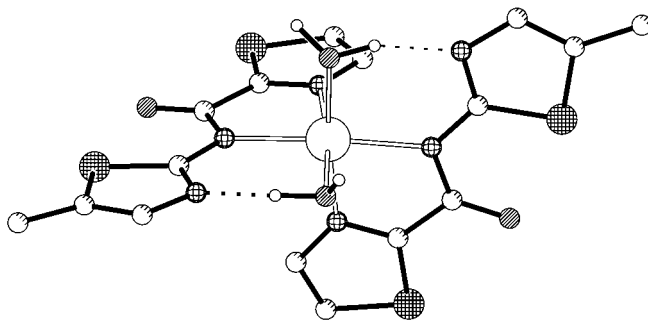
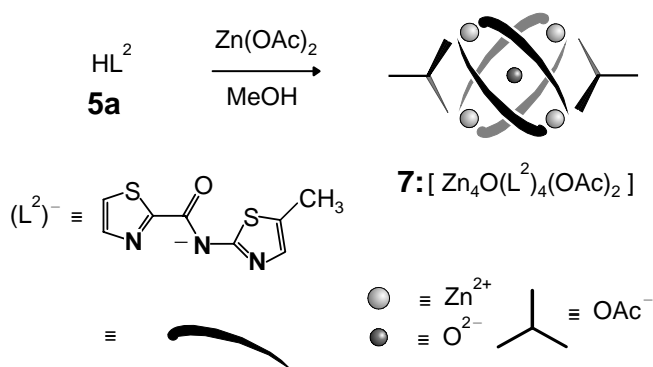


Figure 1. Molecular structure of **6** in the crystal (PLUTON presentation, H atoms are omitted for clarity, except those of water. C: shaded; N: net; O: diagonal; S: mesh; Ni: void).

In contrast, reaction of HL^2 (**5a**) with zinc acetate in methanol yielded colorless crystals of **7**. The elemental analysis and FAB-MS spectrum indicated **7** to be a tetrametallic zinc chelate complex^[5] of the composition $[Zn_4O(L^2)_4(OAc)_2]$ (Scheme 4). 1H and ^{13}C NMR studies of diamagnetic **7** revealed, that all four ligands are chemically identical. However, these data alone did not allow us to unequivocally determine the structure of **7**; therefore, we carried out an X-ray crystallographic structure analysis, which revealed the tetrametallic structure (Figure 2).



Scheme 4. Synthesis of the tetrametallic zinc cluster $[\text{Zn}_4\text{O(L}^2\text{)}_4\text{(OAc)}_2]$ (**7**).

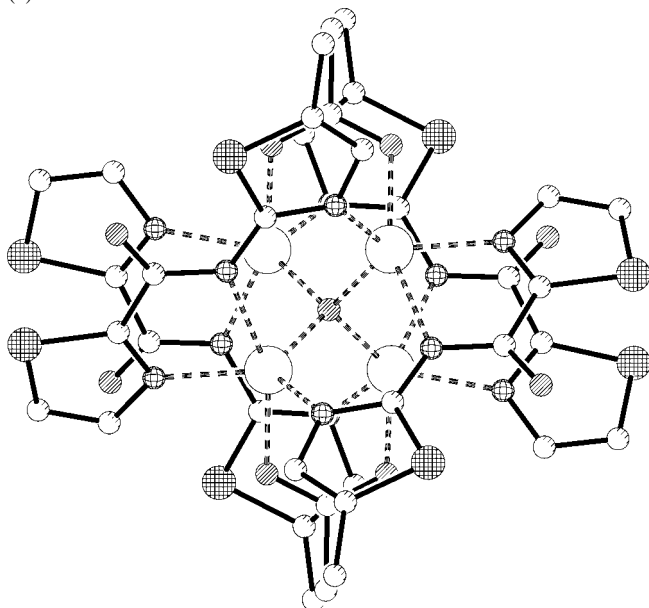


Figure 2. Molecular structure of **7** in the crystal (PLUTON presentation, only one stereoisomer shown). View along one selected C_2 axis, H atoms omitted for clarity. C: shaded; N: net; O: diagonal; S: mesh; Ni: void.

In **7**, the module $[\text{Zn}_2(\text{L}^2)_2]^{2+}$ is generated from two ditopic, tridentate ligands $(\text{L}^2)^-$ and two zinc ions. The two $(\text{L}^2)^-$ ligands coordinate to the zinc ions head-to-tail through the thiazole/amide N-donor groups and the methylthiazole N-donor groups. Two of these building blocks are arranged in such a way that the four zinc ions form the vertices of a tetrahedron. Furthermore, two opposite edges of the D_2 -symmetric module $[\text{Zn}_2(\text{L}^2)_2]^{4+}$ are bridged by two acetate ions, while the two extra opposite edges remain unoccupied to give scaffold $[\{\text{Zn}_2(\text{L}^2)_2\}_2(\text{OAc})_2]^{2+}$. Charge compensation in the final product $[\text{Zn}_4\text{O(L}^2\text{)}_4\text{(OAc)}_2]$ **7** is provided by the central $\mu_4\text{-O}^{2-}$ ion. The overall coordination geometry at the zinc center is square-pyramidal (Figure 3). Dissymmetric **7** crystallizes within the chiral space group $Fdd2$.^[6, 7] Yet, viewed ideally, **7** features D_2 molecule symmetry.

However, when 3-methyl-substituted HL^3 (**5b**) instead of 2-methyl-substituted HL^2 (**5a**) was allowed to react under identical conditions with zinc acetate in methanol, $[\text{Zn}_4\text{O(L}^3\text{)}_4\text{Cl}_2]$ (**8**) was formed and crystallized from dichloromethane. As shown by a single-crystal X-ray structure analysis, **8** is isostructural to $[\text{Zn}_4\text{O(L}^2\text{)}_4\text{(OAc)}_2]$ (**7**). As in **7**, in

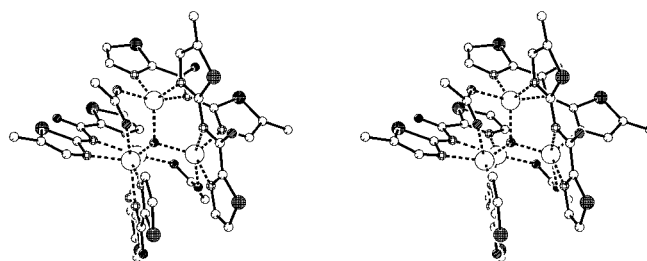
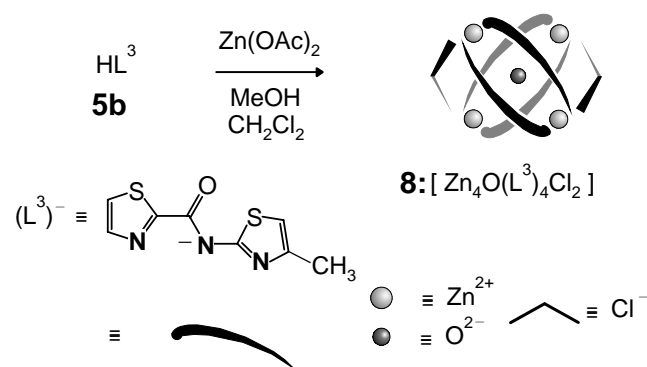


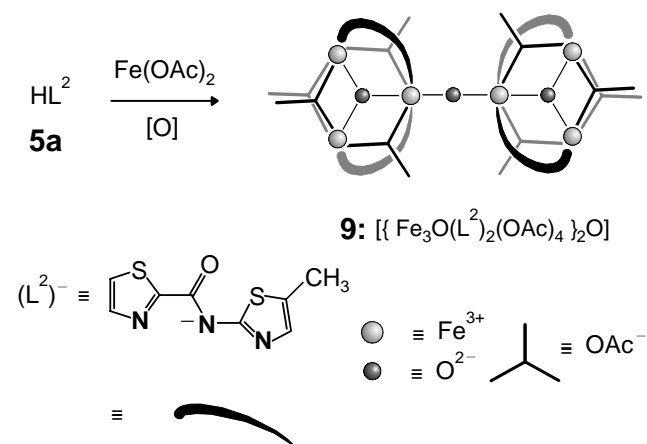
Figure 3. Stereoview of **7** in the crystal (PLUTON presentation, only one stereoisomer shown).

8 two of the edges of the Zn_4 tetrahedron are doubly bridged, two are singly bridged, and the other two are nonbridged. The only difference between **7** and **8** is the exchange of the bridging acetate by chloride ions. The chloride ions in **8** are incorporated during crystallization from dichloromethane (Scheme 5). In contrast to **7**, both enantiomers of D_2 -symmetric **8** crystallize in the centrosymmetric space group $Fddd$.



Scheme 5. Synthesis of the tetrametallic zinc cluster $[\text{Zn}_4\text{O(L}^3\text{)}_4\text{Cl}_2]$ (**8**).

Encouraged by these results, we allowed HL^2 (**5a**) to react with iron(II) acetate under aerobic conditions. After workup a deep red microcrystalline material was isolated. Based on the elemental analysis and the FAB-MS spectrum, **9** is a hexametallc iron(III) chelate complex of the composition $[\text{Fe}_6\text{O}_3(\text{L}^2)_4(\text{OAc})_8]$ (Scheme 6).^[8]



Scheme 6. Synthesis of the hexametallc iron cluster $[\{\text{Fe}_3\text{O(L}^2\text{)}_2(\text{OAc})_4\}_2\text{O}]$ (**9**).

For an unequivocal characterization of **9** a single-crystal X-ray structure determination was carried out (Figure 4). According to this analysis, **9** is composed of two $[\text{Fe}_3\text{O}(\text{L}^2)_2(\text{OAc})_4]^+$ modules, linked by an almost linear μ_2 -oxo bridge ($\text{Fe1}-\mu_2\text{-O}$ 1.78 Å; $\text{Fe1}-\mu_2\text{-O}-\text{Fe4}$ 175.3°). Each of

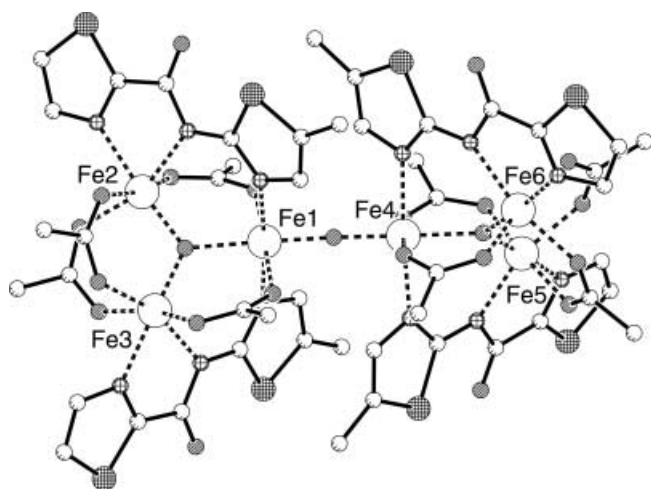


Figure 4. Molecular structure of **9** in the crystal (PLUTON presentation). H atoms omitted for clarity. C: shaded; N: net; O: diagonal; S: mesh; Ni: void.

these two building blocks represents an isosceles triangle with three Fe^{III} ions located in the corners and an $\mu_3\text{-O}^{2-}$ ion in the center ($\text{Fe1}-\mu_3\text{-O}$ 2.05, $\text{Fe2/3}-\mu_3\text{-O}$ 1.85 Å). Two acetate ions link the two Fe^{III} ions of the basic edge ($\text{Fe2}-\text{Fe3}$ 3.17 Å). The two equally long edges are bridged alternating above and below the triangular plane by an acetate and an $(\text{L}^2)^-$ ligand each ($\text{Fe1}-\text{Fe2/3}$ 3.39 Å). As a consequence, all iron(III) ions are coordinated octahedrally. The angle between the two planes of the trimetallic triangles is 84.6°.

The reversible cyclic voltammogram of redox-active **9** was recorded under aprotic conditions and displayed basically three processes attributable to the successive reduction of complex **9** from all- Fe^{III} to all- Fe^{II} (Figure 5, solid line).^[9]

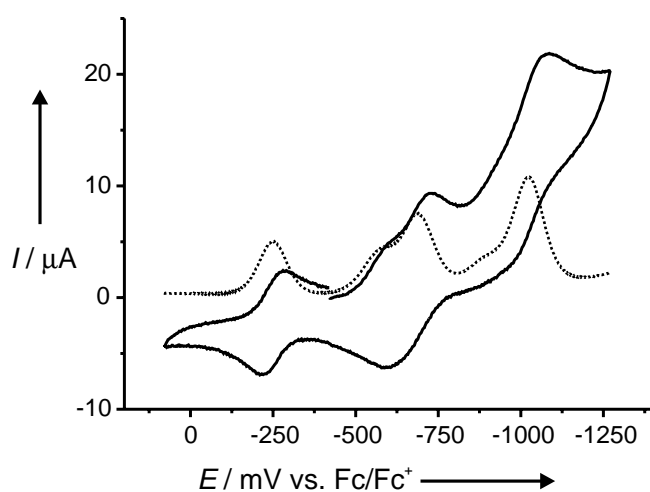


Figure 5. Cyclic voltammogram (solid line) of **9** (thin-layer conditions in CH_2Cl_2 , 0.1 M TBAHFP, scan rate 250 mV^{-1}). Square-wave voltammogram (dotted line) of **9** (pulse height 25 mV, frequency 10 Hz, step increment 2.0 mV) versus Fc/Fc^+ .

Square-wave voltammetry allows better separation of closely lying electrochemical processes and the peak maxima directly display the potentials of the electrochemical processes. With this technique, the number of electrons transferred at different potentials during the reduction of **9** from all- Fe^{III} to all- Fe^{II} was determined in dichloromethane versus Fc/Fc^+ and turned out to be one for the first reduction (-250 mV), two for the second (-610 mV and -700 mV), and three for the third (shoulder at ca. -960 mV and -1040 mV ; Figure 5, dotted line). These findings are evidence for strong coupling across the μ_2 -oxo bridge of the two trimetallic substructures of **9**.

The presence of two different sets of iron(III) ions in **9** was established unequivocally from the Mössbauer spectrum at 77 K. Powder samples of **9** show a quartet, arising from the overlap of two quadrupole doublets (two high-spin $\text{Fe}(1/4)^{\text{III}}$ centers: quadrupolar splitting $\Delta E_{\text{Q}}(77 \text{ K}) = 1.98 \text{ mm s}^{-1}$, isomeric shift $\delta(77 \text{ K}) = 0.55 \text{ mm s}^{-1}$, $\Gamma = 0.27 \text{ mm s}^{-1}$, 33.3%; four high-spin $\text{Fe}(2/3/5/6)^{\text{III}}$ centers: quadrupolar splitting $\Delta E_{\text{Q}}(77 \text{ K}) = 1.01 \text{ mm s}^{-1}$, isomeric shift $\delta(77 \text{ K}) = 0.50 \text{ mm s}^{-1}$, $\Gamma = 0.29 \text{ mm s}^{-1}$, 66.7%; Figure 6).

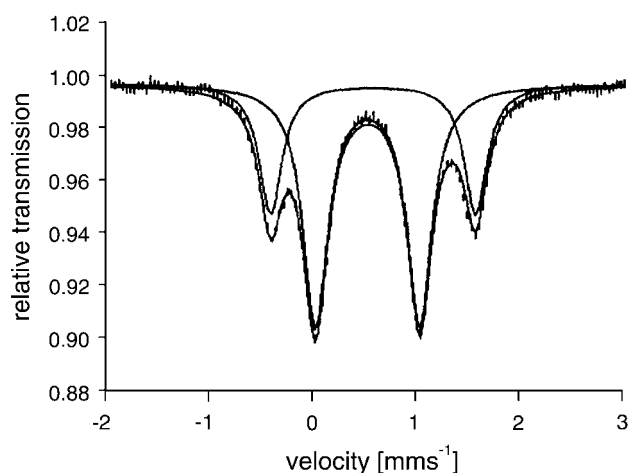


Figure 6. Mössbauer spectrum of a powder sample of $[\{\text{Fe}_3\text{O}(\text{L}^2)_2(\text{OAc})_4\}_2\text{O}]$ (**9**), recorded at 77 K with parameters given in the text. The solid lines are Lorentzian fits.

Conclusion

There is still a long way to go before we are able to reliably predict supramolecular structures. Presently, we are far from understanding the rules governing the generation of mononuclear $[\text{Ni}(\text{L}^2)_2(\text{OH}_2)_2]$ (**6**), tetranuclear $[\text{Zn}_4\text{O}(\text{L}^2)_4(\text{OAc})_2]$ (**7**), or hexanuclear $[\{\text{Fe}_3\text{O}(\text{L}^2)_2(\text{OAc})_4\}_2\text{O}]$ (**9**) complexes, starting from HL^2 and potentially hexacoordinating Ni^{2+} , Zn^{2+} , or Fe^{2+} ions.

Experimental Section

General techniques: Metal salts and reagents were used as obtained from Aldrich. IR spectra were recorded from KBr pellets on a Bruker IFS 25 spectrometer. NMR spectra were recorded on a JEOL JNM-EX-400 spectrometer. All chemical shifts are reported as δ values (ppm) relative to CDCl_3 . FAB-MS spectra were recorded on a Micromass ZAB-Spec

spectrometer. Elemental analyses were performed on a EA 1110 CHNS-Microautomat.

HL² (5a), HL³ (5b)

General method: A suspension of 2/3-methyl-5-aminothiazole (1.14 g, 10 mmol), triethylamine (1.32 g, 13 mmol), and lithium chloride (1.0 g) in anhydrous *N*-methyl-pyrrolidin-2-one was cooled to 0 °C, and 2-thiazolyl chloride^[10] (1.48 g, 10 mmol) was added. The reaction mixture was stirred for three days at 20 °C, water (200 mL) was added and the microcrystalline precipitate was collected on a glass frit. The solid was dried and crystallized from methanol.

HL² (5a): Yield: 2.12 g (94%) bright beige rhombic crystals; m.p. 196 °C; IR (KBr): $\tilde{\nu}$ = 1651, 1555, 1515 cm⁻¹; ¹H NMR (400 MHz, CDCl₃): δ = 2.42 (s, 3H; CH₃), 7.21 (s, 1H; Ar-H), 7.68 (d, 1H; Ar-H), 7.96 (d, 1H; Ar-H), 9.55 ppm (s, 1H; NH); ¹³C NMR (100.5 MHz, CDCl₃): δ = 11.67 (CH₃), 128.24 (Ar-C), 126.00 (Ar-CH), 134.91 (Ar-CH), 144.21 (Ar-CH), 155.89 (Ar-C), 156.98 (Ar-C), 161.27 (C=O); MS (EI, 70 eV): *m/z* (%): 225 (86) [M]⁺; elemental analysis calcd (%) for C₈H₇N₃O₂ (225.30): C 42.65, H 3.13, N 18.65, S 28.47; found: C 42.64, H 3.09, N 18.66, S 28.55.

HL³ (5b): Yield: 1.96 g (87%) bright beige powder; m.p. 171 °C; IR (KBr): $\tilde{\nu}$ = 1673, 1546, 1523 cm⁻¹; ¹H NMR (400 MHz, CDCl₃): δ = 2.32 (s, 3H; CH₃), 6.57 (s, 1H; Ar-H), 7.66 (d, 1H; Ar-H), 7.90 (d, 1H; Ar-H), 10.18 ppm (s, 1H; NH); ¹³C NMR (100.5 MHz, CDCl₃): δ = 16.91 (CH₃), 147.74 (Ar-C), 108.79 (Ar-CH), 126.02 (Ar-CH), 144.18 (Ar-CH), 156.31 (Ar-C), 156.86 (Ar-C), 160.95 (C=O); MS (EI, 70 eV): *m/z* (%): 225 (100) [M]⁺; elemental analysis calcd (%) for C₈H₇N₃O₂ (225.30): C 42.65, H 3.13, N 18.65, S 28.47; found: C 42.87, H 3.10, N 18.50, S 28.37.

[Ni(L²)(H₂O)₂] (6), [Zn₄O(L²)₄(OAc)₂] (7) [Zn₄O(L³)₄Cl₂] (8) and [Fe₃O(L²)₂(OAc)₄]₂O (9)

General method: A solution of HL² (5a) or HL³ (5b) (1.0 mmol) in CH₃OH (20 mL) was added to a solution of metal(II) acetate (0.5 mmol) in CH₃OH (30 mL). The reaction mixture was stirred at 20 °C for 2 h, concentrated to 20 mL, and layered with diethyl ether (10 mL). The precipitate was collected, dried under reduced pressure, and crystallized.

[Ni(L²)(H₂O)₂] (6): Starting material: HL² (5a); yield: 231 mg (85%) dark green prisms from THF/diethyl ether; m.p. > 250 °C (decomp); IR (KBr): $\tilde{\nu}$ = 1602, 1530, 1502 cm⁻¹; FAB-MS (3-nitrobenzyl alcohol (3-NBA)): *m/z* (%): 507 (100) [Ni(L²)₂ - 2H₂O]⁺; elemental analysis calcd (%) for

C₁₆H₁₆N₆O₄S₄Ni (543.29): C 35.37, H 2.97, N 15.47, S 23.61; found: C 36.75, H 3.49, N 14.44, S 23.25.

[Zn₄O(L²)₄(OAc)₂] (7): Starting material: HL² (5a); yield: 236 mg (83%) colorless bipyramids from dichloromethane/diethyl ether; m.p. > 250 °C (decomp); IR (KBr): $\tilde{\nu}$ = 1608, 1574, 1501 cm⁻¹; ¹H NMR (400 MHz, CD₂Cl₂): δ = 1.39 (s, 6H; 2 CH₃CO₂), 2.20 (s, 12H; 4 CH₃), 6.34 (d, 4H; Ar-H), 7.53 (d, 4H; Ar-H), 7.90 (d, 4H; Ar-H); ¹³C NMR (100.5 MHz, CD₂Cl₂): δ = 12.09 (CH₃), 23.25 (CH₃CO₂), 126.13 (Ar-C), 124.78 (Ar-CH), 131.05 (Ar-CH), 132.49 (Ar-CH), 143.10 (Ar-C), 160.53 (Ar-C), 169.61 (C=O), 170.40 (CH₃CO₂); FAB-MS (3-NBA): *m/z* (%): 1232 (35) [Zn₄O(L²)₄(OAc) - OAc]⁺; elemental analysis calcd (%) for C₃₆H₃₀N₁₂O₉S₈Zn₄ (1292.80): C 33.45, H 2.34, N 13.00, S 19.84; found: C 33.38, H 2.37, N 12.64, S 19.21.

[Zn₄O(L³)₄Cl₂] (8): Starting material: HL³ (5b); yield: 217 mg (67%) yellow prisms from dichloromethane/methanol/diethyl ether; m.p. > 250 °C (decomp); IR (KBr): $\tilde{\nu}$ = 1610, 1563, 1499 cm⁻¹; ¹H NMR (400 MHz, CDCl₃): δ = 1.57 (s, 12H; 4 CH₃), 6.28 (s, 4H; Ar-H), 7.47 (d, 4H; Ar-H), 7.93 (d, 4H; Ar-H); ¹³C NMR (100.5 MHz, CDCl₃): δ = 15.95 (CH₃), 108.22 (Ar-C), 124.89 (Ar-CH), 142.73 (Ar-CH), 143.79 (Ar-CH), 160.71 (Ar-C), 169.30 (Ar-C), 170.96 (C=O); FAB-MS (3-NBA): *m/z* (%): 1245 (2) [Zn₄O(L³)₄Cl₂]⁺; elemental analysis calcd (%) for C₃₂H₂₄Cl₂N₁₂O₅S₈Zn₄ (1245.62): C 30.86, H 1.94, N 13.49, S 20.60; found: C 30.45, H 1.89, N 13.33, S 20.34.

[Fe₃O(L²)₂(OAc)₄]₂O (9): Starting material: HL² (5a); yield: 394 mg (45%) dark red rhombic crystals from CHCl₃/diethyl ether; m.p. > 250 °C (decomp); IR (KBr): $\tilde{\nu}$ = 1608, 1574, 1501 cm⁻¹; FAB-MS (3-NBA): *m/z* (%): 1751 (17) [[Fe₃O(L²)₂(OAc)₄]₂O]⁺; elemental analysis calcd (%) for C₄₈H₄₈N₁₂O₁₉S₈Fe₆ (1752.60): C 32.90, H 2.76, N 9.59, S 14.64; found: C 33.25, H 2.75, N 9.58, S 14.57.

Single-crystal X-ray structure analyses: Details of crystal data, data collection, and refinement are given in Table 1. X-ray data were collected on a Nonius Kappa CCD area detector (7, 9) and on a Siemens-P4 diffractometer (6, 8) with MoK α radiation (λ = 0.71073 Å). Lorentz, polarization, and absorption corrections were applied.^[11] The structures were solved by direct methods with SHELXS-97 and refined with full-matrix least-squares against *F*² with SHELXL-97.^[17] All non-hydrogen atoms were refined anisotropically. The hydrogen atoms were fixed in idealized positions using a riding model.

Table 1. Details of X-ray structure determinations.

	6	7	8	9
formula	C ₁₆ H ₁₆ N ₆ O ₄ S ₄ Ni	C ₃₆ H ₃₀ N ₁₂ O ₉ S ₈ Zn ₄	C ₃₂ H ₂₄ Cl ₂ N ₁₂ O ₅ S ₈ Zn ₄ · CH ₂ Cl ₂ · H ₂ O	C ₄₈ H ₄₈ N ₁₂ O ₁₉ S ₈ Fe ₆ · CHCl ₃ · (CH ₃ CH ₂) ₂ O
<i>M_r</i>	543.29	1292.80	1348.43	1946.02
crystal size [mm]	0.60 × 0.50 × 0.40	0.30 × 0.20 × 0.20	0.35 × 0.22 × 0.16	0.35 × 0.30 × 0.20
crystal system	monoclinic	orthorhombic	orthorhombic	monoclinic
space group	<i>P</i> 2(1)/ <i>c</i>	<i>F</i> dd2	<i>F</i> ddd	<i>C</i> 2/ <i>c</i>
<i>T</i> [K]	210(2)	173(2)	210	173(2)
<i>a</i> [Å]	12.656(4)	21.2555(9)	11.986(2)	24.4372(3)
<i>b</i> [Å]	14.760(5)	42.8109(13)	19.492(2)	13.2889(2)
<i>c</i> [Å]	12.203(4)	13.5612(6)	46.895(6)	26.9201(3)
α [°]	90	90	90	90
β [°]	113.37(2)	90	90	95.5410(10)
γ [°]	90	90	90	90
<i>V</i> [Å ³]	2093(2)	12340.2(8)	10956(3)	8701.28(19)
<i>Z</i>	4	8	8	4
ρ_{calcd} [Mg m ⁻³]	1.725	1.392	1.635	1.635
θ range [°]	1.75 to 27.01	2.28 to 25.02	2.04 to 25.00	1.52 to 27.48
reflections collected	5595	5255	4576	16733
unique reflections	4560	5255	2425	9910
[<i>R</i> _{int}]	0.0609	0	0.1193	0.0320
refl. observed [<i>I</i> > 2 σ (<i>I</i>)]	3280	4708	1253	6868
parameters	329	330	170	519
absorption correction method	none	Psi-scans	Psi-scans	Scapecack
final <i>R</i> 1 [<i>I</i> > 2 σ (<i>I</i>)]	0.0513	0.0742	0.0726	0.0496
<i>wR</i> 2 (all data)	0.1358	0.2135	0.1755	0.1601
largest residuals [e Å ⁻³]	0.505/ - 0.878	1.594/ - 0.853	0.802/ - 0.432	1.473/ - 0.733

CCDC-174359 (6), CCDC-174592 (7), CCDC-174360 (8), and CCDC-174591 (9) contain the supplementary crystallographic data for the structures reported in this paper. These data can be obtained free of charge via www.ccdc.cam.ac.uk/conts/retrieving.html (or from the Cambridge Crystallographic Data Centre, 12 Union Road, Cambridge CB2 1EZ, UK; fax: (+44) 1223-336033; or deposit@ccdc.cam.ac.uk).

Acknowledgement

This work was supported by the Deutsche Forschungsgemeinschaft Sa 276/25–1, SFB 583, GK 312, the Bayerisches Langzeitprogramm Neue Werkstoffe, and the Fonds der Chemischen Industrie. M. B. thanks the Studienstiftung des Deutschen Volkes for a Ph.D. fellowship. The generous allocation of X-ray facilities by Professor D. Sellmann, Institut für Anorganische Chemie, Universität Erlangen-Nürnberg, is also gratefully acknowledged. Finally, we are grateful to one of the referees for bringing an error in one of the cartoons to our attention.

- [1] J.-M. Lehn, *Supramolecular Chemistry*, Wiley-VCH, Weinheim, **1995**; J.-M. Lehn, *Angew. Chem.* **1988**, *100*, 91–116; *Angew. Chem. Int. Ed. Engl.* **1988**, *27*, 89–112.
- [2] Recent reviews: B. J. Holliday, C. A. Mirkin, *Angew. Chem.* **2001**, *113*, 2076–2097; *Angew. Chem. Int. Ed.* **2001**, *40*, 2022–2043; S. Leininger, B. Olenyuk, P. J. Stang, *Chem. Rev.* **2000**, *100*, 853–908; R. W. Saalfrank, B. Demleitner in *Transition Metals in Supramolecular Chemistry* (Ed.: J. P. Sauvage), Wiley-VCH, Weinheim, **1999**, p. 1–51; E. Uller, B. Demleitner, I. Bernt, R. W. Saalfrank in *Structure and Bonding*, Springer, Berlin, **2000**, Vol. 96 (Ed.: M. Fujita), p. 149–175; D. L. Caulder, K. N. Raymond, *Acc. Chem. Res.* **1999**, *32*, 975–982; J. L. Atwood, L. R. MacGillivray, *Angew. Chem.* **1999**, *111*, 1080–1096; *Angew. Chem. Int. Ed.* **1999**, *38*, 1018–1033; M. Fujita, *Chem. Soc. Rev.* **1998**, *27*, 417–425; C. J. Jones, *Chem. Soc. Rev.* **1998**, *27*, 289–299; D. Philp, J. F. Stoddart, *Angew. Chem.* **1996**, *108*, 1242–1286; *Angew. Chem. Int. Ed. Engl.* **1996**, *35*, 1154–1196; S. L. James, M. P. Mingos, A. J. P. White, D. J. Williams, *Chem. Commun.* **1998**, *21*, 2323–2324; P. N. W. Baxter in *Comprehensive Supramolecular Chemistry*, Vol. 9 (Ed.: J.-M. Lehn), Pergamon, Oxford, **1996**, p. 165–211; E. C. Constable in *Comprehensive Supramolecular Chemistry*, Vol. 9 (Ed.: J.-M. Lehn), Pergamon, Oxford, **1996**, p. 43–83; C. Piguet, G. Bernardinelli, G. Hopfgartner, *Chem. Rev.* **1997**, *97*, 2005–2062; M. Ruben, E. Breuning, J.-P. Gisselbrecht, J.-M. Lehn, *Angew. Chem.* **2000**, *112*, 4312–4315; *Angew. Chem. Int. Ed.* **2000**, *39*, 4139–4142; E. Breuning, M. Ruben, J.-M. Lehn, F. Renz, Y. Garcia, V. Ksenofontov, P. Gütllich, E. Wegelius, K. Rissanen, *Angew. Chem.* **2000**, *112*, 2563–2566; *Angew. Chem. Int. Ed.* **2000**, *39*, 2504–2507; D. W. Johnson, K. N. Raymond, *Supramolecular Chem.* **2001**, *13*, 639–659; G. F. Swiegers, T. J. Malefetse, *Coordination Chemistry Rev.* **2002**, *225*, 91–121.
- [3] R. W. Saalfrank, S. Trummer, U. Reimann, M. M. Chowdhry, O. Waldmann, *Angew. Chem.* **2000**, *112*, 3634–3636; *Angew. Chem. Int. Ed.* **2000**, *39*, 3492–3494.
- [4] A. G. Oertli, W. R. Meyer, U. W. Suter, F. B. Joho, V. Gramlich, W. Petter, *Helv. Chim. Acta* **1992**, *75*, 184–189.
- [5] See: A. F. Cotton, L. M. Daniels, L. R. Falvello, J. H. Matonic, C. A. Murillo, X. Wang, H. Zhou, *Inorg. Chim. Acta* **1997**, *266*, 91–102; L. Hiltunen, M. Leskelä, M. Mäkelä, L. Niinistö, *Acta Chem. Scand. A* **1987**, *41*, 548–555; C.-F. Lee, K.-F. Chin, S.-M. Peng, C.-M. Che, *J. Chem. Soc. Dalton Trans.* **1993**, 467–470.
- [6] The structure of **7** was refined as a racemic twin according to standard procedures implemented and described within the SHELX-97 refinement package.^[7]
- [7] G. M. Sheldrick, SHELXS-97, Program for the Solution of Crystal Structures, University of Göttingen, **1997**; G. M. Sheldrick, SHELXL-97, Program for the Refinement of Crystal Structures, University of Göttingen, **1997**; H. D. Flack, *Acta Crystallogr. Sect. A* **1983**, *39*, 876–881.
- [8] For other iron(III) acetate complexes, see: C. T. Dziobkowski, J. T. Wroblewski, D. B. Brown, *Inorg. Chem.* **1981**, *20*, 671–678; E. M. Holt, S. L. Holt, W. F. Tucker, R. D. Asplund, K. L. Watson, *J. Am. Chem. Soc.* **1974**, *96*, 2621–2623; S. M. Head, E. A. Stern, B. Bunker, E. M. Holt, S. L. Holt, *J. Am. Chem. Soc.* **1979**, *101*, 67–73; C. J. Harding, R. K. Henderson, A. K. Powell, *Angew. Chem.* **1993**, *105*, 583–585; *Angew. Chem. Int. Ed. Engl.* **1993**, *32*, 570–572; D. F. Harvey, C. A. Christmas, J. K. McCusker, P. M. Hagen, R. K. Chadha, D. N. Hendrickson, *Angew. Chem.* **1991**, *103*, 592–594; *Angew. Chem. Int. Ed. Engl.* **1991**, *30*, 598–600; J. K. McCusker, C. A. Christmas, P. M. Hagen, R. K. Chadha, D. F. Harvey, D. N. Hendrickson, *J. Am. Chem. Soc.* **1991**, *113*, 6114–6124; C. A. Christmas, H.-L. Tsai, L. Pardi, J. M. Kesselman, P. K. Gantzel, R. K. Chadha, D. Gatteschi, D. F. Harvey, D. N. Hendrickson, *J. Am. Chem. Soc.* **1993**, *115*, 12483–12490; I. Shwey, L. E. Pence, G. C. Papaefthymiou, R. Sessoli, J. W. Yun, A. Bino, S. J. Lippard, *J. Am. Chem. Soc.* **1997**, *119*, 1037–1042.
- [9] Amel System 5000. Ungraduated cell with Pt plate electrodes and pseudoreference electrode. Potential measured versus Fc/Fc⁺. M. Büschel, C. Stadler, C. Lambert, M. Beck, J. Daub, *J. Electroanal. Chem.* **2000**, *484*, 24–32; R. W. Saalfrank, S. Trummer, H. Krautscheid, V. Schünemann, A. X. Trautwein, S. Hien, C. Stadler, J. Daub, *Angew. Chem.* **1996**, *108*, 2350–2352, *Angew. Chem. Int. Ed. Engl.* **1996**, *35*, 2206–2208.
- [10] P. Jutzli, U. Gilge, *J. Heterocyclic Chem.* **1983**, *20*, 1011.
- [11] “Collect” data collection software, Nonius B. V., **1998**; “Scalepack” data processing software: Z. Otwinowski, W. Minor, *Method Enzymol.* **1997**, *276*, 307.
- [12] R. W. Saalfrank, B. Demleitner, H. Glaser, H. Maid, D. Bathelt, F. Hampel, W. Bauer, M. Teichert, *Chem. Eur. J.* **2002**, *8*, 2679–2683.

Received: January 29, 2002 [F 3833]